# SILICA SUPPORTED WO₃/CU₂O HETEROSTRUCTURED NANOPARTICLES FOR PHOTOCATALYTIC DEGRADATION OF HORMONES

*Hassan ALI, Milan MASAR, Muhammad YASIR, Tomas SOPIK, Pavel URBANEK, Michal MACHOVSKY, Ivo KURITKA

*Centre of Polymer Systems, Tomas Bata University in Zlin, Zlin, Czech Republic, EU, hali@utb.cz*

## Abstract

In this study, a WO₃/Cu₂O based heterojunction was synthesized via a facile solvothermal method. The as-prepared nanocomposite was characterized by XRD, SEM, and UV-vis spectroscopy. The photocatalytic activity of the as-prepared heterojunction was evaluated by the means of estradiol (E2) and 17α-ethinylestradiol (EE2) hormone degradation under UV LED illumination wavelength at $\lambda_{max} \sim$ 365 nm. The degradation results showed that the prepared photocatalyst was able to achieve considerable photoactivity owing to the intrinsic heterojunction charge transfer mechanism. Photocatalytic degradation rates of 27 and 35 % were achieved for the E2 and EE2 hormones, respectively.

**Keywords:** WO₃/Cu₂O, heterojunction, degradation, photocatalysis, estrogens

## 1.    INTRODUCTION

Over the last few decades, extensive use of chemicals and its production on industrial scale have resulted in serious environmental and ecological issues, mainly due to the contamination of aqueous resources vital for sustaining the life cycle [1]. Among the commonly discharged chemical affluents, pharmaceuticals like antibiotics and hormonally active agents, also classified as endocrine-disrupting chemicals (EDC) are of particular importance due to relatively high bio toxicity, even at minuscule concentrations [2]. The elimination of these chemical toxicants including EDC is imperative since the exposure of such chemicals are associated with several chronic diseases such as cancer, ADHD, learning disability, brain development and retarded sexual development. Therefore, it is imperative to develop sustainable water treatment systems capable of eliminating these toxic chemicals with low cost and energy requirements. So far, various strategies have been implemented to address this issue, including adsorption, biological degradation, electrochemical oxidation (EO), membrane technology, sonolysis, and photocatalysis, each having specific advantages and disadvantages [3,4]. For example, frequent replacement of electrodes and membranes due to fouling increases the operational costs of EO and membrane filtration techniques, respectively [5]. Photocatalysis, in this regard, is currently considered the most sustainable method and has been employed in various applications such as pollutants removal, fuel generation, pathogen elimination, and nitrogen fixation [6–8]. A typical photocatalysis process requires only a suitable semiconductor photocatalyst, reaction medium and solar light irradiation as an energy input. The process is initiated by the absorption of photons having energy equal to or greater than the bandgap of the photocatalyst. This results in the excitation of the electrons in the valence band (VB) to the conduction band (CB) and subsequent generation of electron-hole pairs. These excited electrons and holes then participate in the reduction and oxidation of the water molecules and the adsorbed chemical species on the surface of the photocatalyst. However, currently developed photocatalysts suffer from several critical issues which limit their photoactivity, i.e., the wide bandgap of commonly used photocatalysts results in poor visible light harvesting and futile recombination of the generated photoexcited charge carriers [8]. To address these fundamental drawbacks, several modification strategies have been implemented so far to-date such as surface engineering, sensitization, defect engineering, doping, and

heterojunction [9,10]. Out of these, the construction of heterojunction has compelling advantages of addressing the previously mentioned issues associated with the single component photocatalysts, namely, the suppression of charge recombination and extension of light absorption to visible range. Numerous heterojunctions systems have been investigated so far with promising photocatalytic activities [11]. Among several dual photocatalytic systems, construction of $WO_3$ and $Cu_2O$ based heterojunction presents an attractive approach primarily due to favorable to band position.

## 2. EXPERIMENTAL

### 2.1. Materials

Hydrogen peroxide ($H_2O_2$) (Lachner), copper(II) sulfate ($CuSO_4$) (Lachner), glucose ($C_6H_{12}O_6$) (Lachner), and sodium hydroxide (NaOH) (Lachner) were used for the preparations of the sample. The tungsten powder was obtained from ISS Nippon Kayaku group. Estradiol (E2) and 17α-ethinylestradiol (EE2) were purchased from Sigma-Aldrich, Germany. All chemicals were of analytic grade with p.a. ≥ 99.5 % and were used as received without further purification. All aqueous solutions were prepared by demineralized water.

### 2.2. Synthesis of $WO_3/Cu_2O$ nanocrystals

In the first step, $WO_3$ was prepared from starting solution of peroxotungstic acid ($[WO_2(O_2)H_2O]\cdot nH_2O$, PTA) which was obtained by dissolving 1 g of tungsten powder in 20 mL of $H_2O_2$. Tungsten powder dissolved quickly under intense stirring and at elevated temperature (55-60°C). Next, 5 g of silica was added into the prepared starting solution, and by a Teflon stick thoroughly mixed to the resulting paste. This paste was dried at 45 °C for 24 hours. The as-prepared powder was crushed in a mortar with a pestle. Subsequently, this powder was annealed for 2 hours at 550 °C in a muffle furnace. The obtained $WO_3$ powder prepared by this synthesis method was used in the next step for $Cu_2O$ decoration as follows: 300 mg of previously prepared $WO_3$ powder and 8 mL of ammonia solution with 75 mg of $CuSO_4$ were mixed with a magnetic stirrer. After a short time, 150 mg of glucose was added with continuous stirring, followed by adjusting pH of the mixture with NaOH.

### 2.4. Characterization methods

Phase structure of all samples was investigated by XRD diffractometer MiniFlex600 (Japan, RIGAKU) with a Co-Kα X-ray source (λ = 1.7903 Å) in the diffraction angle range of 5-90° 2θ. Crystallite sizes were estimated according to the Scherrer's equation as follows:

$$d = K\lambda/\beta cos\theta \tag{1}$$

where $d$ is the diameter and the shape factor $K$ is 0.89, since no preferential orientation was observed, $\lambda$ is the wavelength (CoKα 1,2) = 0.179 nm, the angle θ is the full width half maximum FWHM of the corresponding highest diffraction peak, i.e., (002) and (111) line for $WO_3$ and $Cu_2O$, respectively, and β is the line broadening at half the maximum intensity corrected for the instrumental response. Sample analysis was performed by NovaNanoSEM 450 microscope (The Netherland, FEI company). Microscopic images were taken using an ETD (topographic contrast) and CBS (material contrast) detector accelerated at 5 kV and 15 kV voltages.

### 2.5. Photocatalytic experiment

The photocatalytic adsorption and degradation experiment was performed using $WO_3/Cu_2O$ as a photocatalyst in an aqueous mixture of hormone solution containing E2 and EE2 hormones. Each photocatalytic test was conducted by transferring 5 mg of the powdered catalyst into a beaker containing 10 mL of hormone solution with each hormone at a concentration of 0.2 mg/L and a total solution concentration of 0.8 mg/L. Separate beakers were used to evaluate the hormones adsorption rate under constant magnetic stirring at 450 rpm. Additionally, a separate beaker containing solution only was kept as a reference to calculate the removal

percentage from the initial concentration. Results were obtained from high-performance liquid chromatography (HPLC) using calibration after running each sample twice.

### 2.6. HPLC Method

HPLC analysis was performed on a Dionex UltiMate 3000 Series equipped with a diode array detector (Thermo Fisher Scientific, Germany) according to the previously reported technique [12]. The concentration of hormones was calculated from the results of the 200 nm performed test (concentration of calibration standards 0.20 – 0.02 mg/L; Data were recorded and processed in Chromeleon 7.2 software (Thermo Fisher Scientific) [13].

### 3. RESULTS AND DISCUSSION

The crystalline phase structures of the $WO_3$/$Cu_2O$ heterojunction are shown in **Figure 1**. For reference, peroxotungstic acid (PTA) and silica-supported $WO_3$ diffractograms are also given. The XRD pattern of the PTA exhibits intense peaks in the range of small Braggs angles, typically associated with layered compounds. The as-prepared silica supported $WO_3$ exhibits several characteristic peaks, indexed to (002), (020), (200), (112), (202), (220), (222), (004), (040), (223), and (402) planes as reported in PDF Card No. 01-071-4310. From **Figure 1c**, it can be seen that the characteristic peaks of $Cu_2O$, corresponding to the (111), (200), (220), (311) planes appeared as reported in PDF card No. 01-071-0305, indicating successful formation of the heterojunction. The peaks are broader and of low intensity due to the presence of silica. Moreover, the decrease of signal intensity for $WO_3$ is observed which can be attributed due to possible shielding of newly formed cupric crystalline phase. No other crystalline phases such as $CuWO_4$ were detected in the samples. The average crystallite sizes of the $WO_3$ and $Cu_2O$ were calculated to be 57.64 and 50.24 nm, respectively, according to Scherrer's formula.
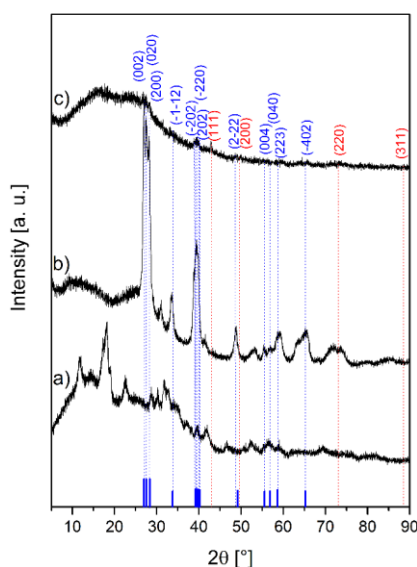


**Figure 1** XRD patterns for silica treated by peroxotungstic acid precursor (a), silica-supported $WO_3$ obtained by calcining precursor at 550 °C (b) and silica-supported $WO_3$/$Cu_2O$ heterostructure.

The morphology of the as-prepared samples was investigated using SEM as shown in **Figure 2**. The SEM images of silica-supported PTA precursor exhibits course morphology with small grain size, which is consistent with poor crystallinity as evidenced by the XRD results (**Figure 2A-B**). For the annealed samples, $WO_3$ and $WO_3$/$Cu_2O$, an increase in the temperature led to smaller grain size and a large number of $Cu_2O$ particles were observed on the surface of the $WO_3$ embedded with silica. No agglomeration of $Cu_2O$ particles was noticed.
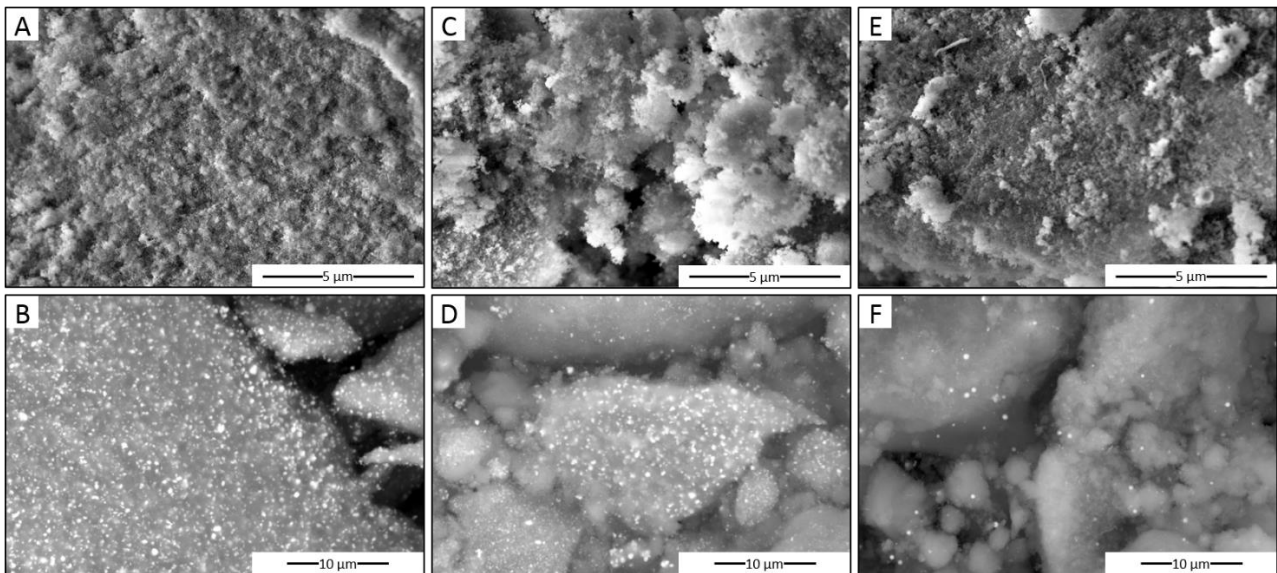
**Figure 2** SEM images of peroxotungstic acid precursor (A-B), silica-supported $WO_3$ (C-D), and silica-supported $WO_3/Cu_2O$ heterojunction (E-F). Top and bottom images were taken by ETD and CBS detector, respectively.

The electronic structure of semiconductor which plays a crucial role in the photoactivity is closely related to its bandgap and its alignment. The as-prepared $WO_3/Cu_2O$ sample was also characterized by UV-vis analysis to evaluate the optical bandgap value via Kubelka-Munk equation, as previously reported [14].

$$[\alpha h\nu]^p = A(h\nu - Eg) \tag{2}$$

where $\alpha$ is the optical absorption coefficient, $h\nu$ stands for quantized photon energy, $A$ is the constant of proportionality, and the value $p$ indicates the electronic transition type. The value of the exponent, $p$, was determined by plotting a $[F(R){\cdot}h\nu]^{1/2}$ vs $h\nu$ graph and calculating the best fit, which turned out to be ½, implying an indirect allowed transition. Finally, by plotting a $[F(R){\cdot}h\nu]^{1/2}$ vs $h\nu$ graph and extrapolation of the graph slope to $F(R) \rightarrow 0$, the optical bandgap values were obtained as shown in **Figure 4**.
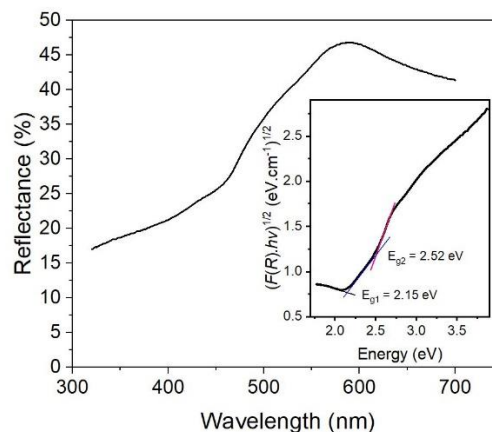


**Figure 4** Reflectance spectrum and the calculated bandgap energies (inset) of the silica-supported $WO_3/Cu_2O$ composite.

The photocatalytic activity of the as-prepared nanocomposite was evaluated via E2 and EE2 hormones degradation having an initial concentration of 0.2 mg/L under UV light irradiation (Roithner LaserTechnik,

UVLUX 340-HL-3) with a maxima wavelength of 343 nm (corresponding to $E_g \sim 3.6$ eV). From **Figure 5**, it is obvious that the photocatalytic activity gradually increased with increasing time, reaching 26 and 35 % after 1 h duration, for E2 and EE2, respectively. However, it should be noted that the reference sample without light irradiation also recorded some hormonal removal due to adsorption, with contribution reaching as high as 5.4 (E2) and 7.8 % (EE2), within 1 h duration. This high degree of hormonal adsorption could be ascribed due to the presence of a large number of silica particles, possessing highly porous structure and large surface area.
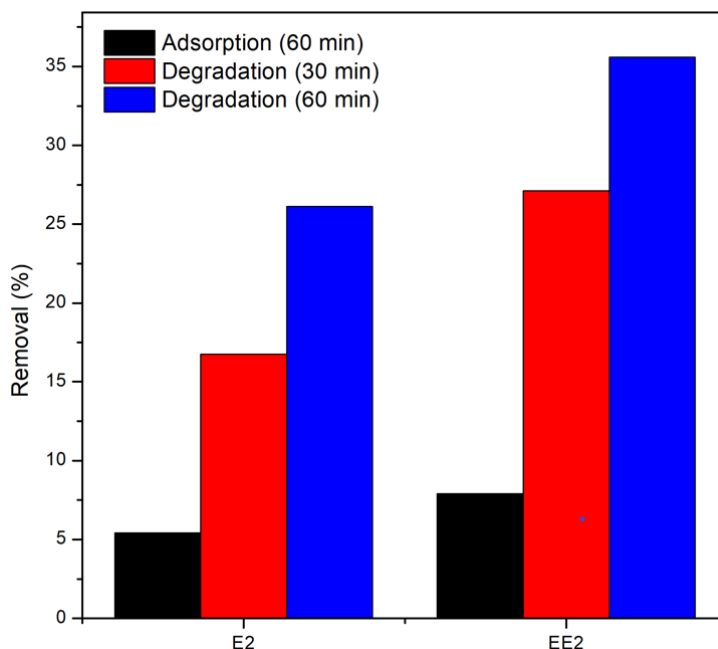


**Figure 5** Photocatalytic and adsorption activity of $WO_3/Cu_2O$ heterojunction

## 4.    CONCLUSION

A silica supported $WO_3/Cu_2O$ heterojunction was prepared via a facile solvothermal method employing peroxotungstic acid and copper sulfate as precursors. XRD and SEM analysis showed the formation of a suitable heterojunction was successful. The as-prepared $WO_3/Cu_2O$ showed significant photocatalytic activity towards estrogenic hormonal degradation under UV light irradiation. The enhanced photoactivity was attributed due to the advantageous charge transfer route of heterojunction. This work may provide insights into developing new highly efficient materials for environmental pollutants degradation.

**REFERENCES**

[1]    ARYAL, N., WOOD, J., RIJAL, I., DENG, D., JHA, M. K., OFORI-BOADU, A. Fate of environmental pollutants: A review. *Water Environment Research.* 2020, vol. 92, no. 10, pp. 1587–94. Available from: https://doi.org/doi.org/10.1002/wer.1404.

[2]    LA MERRILL, M. A., VANDENBERG, L. N., SMITH, M. T., GOODSON, W., BROWNE, P., PATISAUL, H. B.,

GUYTON, K. Z., KORTENKAMP, A., COGLIANO, V. J., WOODRUFF, T. J., RIESWIJK, L., SONE, H., KORACH, K. S., GORE, A. C., ZEISE, L., ZOELLER, R. T. Consensus on the key characteristics of endocrine-disrupting chemicals as a basis for hazard identification. *Nature Reviews Endocrinology.* 2020, vol. 16, no. 1, pp. 45–57. Available from: https://doi.org/10.1038/s41574-019-0273-8.

[3]    KUMAR, S., AHLAWAT, W., BHANJANA, G., HEYDARIFARD, S., NAZHAD, M. M., DILBAGHI, N. Nanotechnology-based water treatment strategies. *Journal of Nanoscience and Nanotechnology.* 2014, vol. 14, no. 2, pp. 1838–1858. Available from: https://doi.org/10.1166/jnn.2014.9050.

[4]    UDDIN, Z., AHMAD, F., ULLAN, T., NAWAB, Y., AHMAD, S., AZAM, F., RASHEED, A., ZAFAR, M. S. Recent trends in water purification using electrospun nanofibrous membranes. *International Journal of Environmental Science and Technology.* 2021. Available from: https://doi.org/10.1007/s13762-021-03603-9.

[5]    JAFARI, M., VANOPPEN, M., VAN AGTMAAL, J. M. C., CORNELISSEN, E. R., VROUWENVELDER, J. S., VERLIEFDE, A., VAN LOOSDRECHT, M. C. M., PICIOREANU, C. Cost of fouling in full-scale reverse osmosis and nanofiltration installations in the Netherlands. *Desalination.* 2021, vol. 500, article no. 114865. Available from: https://doi.org/10.1016/j.desal.2020.114865.

[6]    GAO, Y., DUAN, J., ZHAI, X., GUAN, F., WANG, X., ZHANG, J., HOU, B. Photocatalytic Degradation and Antibacterial Properties of Fe3+-Doped Alkalized Carbon Nitride. *Nanomaterials.* 2020, vol. 10, no. 9, pp. 1751. Available from: https://doi.org/10.3390/nano10091751.

[7]    ALI, H., MASAR, M., GÜLER, A. C. C., URBÁNEK, M., MACHOVSKY, M., KUŘITKA, I. Heterojunction-based photocatalytic nitrogen fixation: Principles and current progress. *Nanoscale Advances.* 2021, vol. 3, no. 22, pp. 6358–6372. Available from: https://doi.org/10.1039/D1NA00565K.

[8]    DJURIŠIĆ, A. B., HE, Y., NG, A. M. C. Visible-light photocatalysts: Prospects and challenges. *APL Materials.* 2020, vol. 8, no. 3, pp. 030903. Available from: https://doi.org/10.1063/1.5140497.

[9]    XIONG, L., TANG, J. Strategies and Challenges on Selectivity of Photocatalytic Oxidation of Organic Substances. *Advanced Energy Materials.* 2021, vol. 11, no. 8, pp. 2003216. Available from: https://doi.org/10.1002/aenm.202003216.

[10]   SAPUTERA, W. H., RIZKIANA, J., WULANDARI, W., SASONGKO, D. Role of defects on TiO2/SiO2composites for boosting photocatalytic water splitting. *RSC Advances.* 2020, vol. 10, no. 46, pp. 27713-27719. Available from: https://doi.org/10.1039/d0ra05745b.

[11]   NADEEM, M. A., KHAN, M. A., ZIANI, A. A., IDRISS, H. An overview of the photocatalytic water splitting over suspended particles. *Catalysts.* 2021, vol. 11, no. 1, pp. 60. Available from: https://doi.org/10.3390/catal11010060.

[12]   YASIR, M., ŠOPÍK, T., KIMMER, D., SEDLAŘÍK, V. Facile HPLC technique for simultaneous detection of estrogentic hormones in wastewater In: *NANOCON 2020 Conference Proceedings.* Brno: Nanocon, 2020, pp. 272–276. Available from: https://doi.org/10.37904/nanocon.2020.3710.

[13]   YASIR, M., ŠOPÍK, T., LOVECKÁ, L., KIMMER, D., SEDLAŘÍK, V. The adsorption, kinetics, and interaction mechanisms of various types of estrogen on electrospun polymeric nanofiber membranes. *Nanotechnology.* 2022, vol. 33, no. 7, pp. 075702. Available from: https://doi.org/10.1088/1361-6528/ac357b.

[14]   ALI, H., GULER, A. C., MASAR, M., URBANEK, P., URBANEK, M., SKODA, D., SULY, P., MACHOVSKY, M., GALUSEK, D., KURITKA, I. Solid-State Synthesis of Direct Z-Scheme $Cu_2O/WO_3$ Nanocomposites with Enhanced Visible-Light Photocatalytic Performance. *Catalysts.* 2021, vol. 11, no. 2, pp. 1–26. Available from: https://doi.org/10.3390/catal11020293.